Reflection of Cluster Beams on Metal Surfaces: Momentum and Heat Transfer

H. Mayer

Blocksberg 25, D-21465 Reinbek

Z. Naturforsch. **53a,** 663–669 (1998); received March 8, 1998

Beams of clusters, the latter containing about 10^6 nitrogen molecules, were reflected by polished metal surfaces, and the direction, the velocity and the composition of the reflected beams were studied as functions of the direction of the incident beam. It turned out that the clusters leave the reflector surface almost tangentially, with reduced velocity, and that besides the clusters the beams contain gaseous nitrogen formed during the impact.

Key words: Cluster Beams; Molecular Beams; Beam Surface Interaction; Cluster Reflection; Heat Transfer.

1. Introduction

Molecular beams with the majority of the molecules forming agglomerates ("clusters") are termed cluster beams. Cluster beams are generated by supersonic expansion of a gas out of a Laval nozzle and subsequent transfer of the beam core into high vacuum [1, 2]. Such beams can be used for fuel injection in nuclear fusion devices [3]. In this and other contexts it is of interest to know how the clusters behave when reflected by solid surfaces.

Appropriate experiments [4–11] have shown that cluster beams, when reflected by polished surfaces, still consist mainly of clusters. Thus, it is possible to enhance the flux density of cluster beams by reflection [4, 5]. The reflection characteristics depend on the cluster size*, the incident angle [4, 5], the temperature of the reflector [4–8], and its surface structure [11]. Using sufficiently large clusters, the influence of the surface structure becomes negligible.

The present paper reports on the reflection of nitrogen clusters which contain about 10^6 molecules. The reflector remains at room temperature and its surface roughness should not influence the beam. The measurements are for the first time supplemented by momentum and heat transfer investigations performed at the reflector. In accordance with prior experiments [4, 5], the direction and velocity of the reflected beam is found to practically agree with the tangential component of the velocity of the incident beam. Due to the vanishing normal velocity, the flux density (definition: N_2-molecules per time unit and area unit) of the reflected beam is enhanced as compared to that of the incident beam. The assumption of previous considerations [4, 5], that the loss of kinetic energy causes partial evaporation of the clusters is confirmed by the size evaluations performed here; however, the present heat transfer measurements show that part of the required heat of evaporation is taken from the reflector.

According to the measurements also the evaporated molecules leave the reflector almost without normal velocity. This phenomenon can be explained by the assumption that during the reflection the surfaces of the clusters and of the reflector form a gap out of which the gas generated by evaporation effuses mainly parallel to the reflector surface.

2. Experimental

The experimental setup is shown schematically in Figure 1.1. For measurements of the flux density it consists of the beam generating system, the reflector and an ionization gauge tube. For velocity and size measurements a fast rotating chopper disk is mounted above the reflector and a mass analyzer substitutes the gauge tube.

The beam gas used is a mixture of 20 mole% nitrogen and 80 mole% hydrogen. By addition of hydrogen as a condensation agent, being almost completely eliminated from the cluster beam prior to its arrival in the high vacuum chamber, the flux density is considerably enhanced [2]. Through a conical nozzle (1 mm diameter at the nar-

* "Cluster size": The ratio of the mean number of molecules n to the number of elementary charges z is called the cluster size. The cluster charge is limited to few elementary charges [14].

Reprint requests to Prof. H. Mayer, Fax: 040 722 78 53.

0932-0784 / 98 / 0800-0663 $ 06.00 © – Verlag der Zeitschrift für Naturforschung, D-72027 Tübingen

Dieses Werk wurde im Jahr 2013 vom Verlag Zeitschrift für Naturforschung in Zusammenarbeit mit der Max-Planck-Gesellschaft zur Förderung der Wissenschaften e.V. digitalisiert und unter folgender Lizenz veröffentlicht: Creative Commons Namensnennung-Keine Bearbeitung 3.0 Deutschland Lizenz.

This work has been digitalized and published in 2013 by Verlag Zeitschrift für Naturforschung in cooperation with the Max Planck Society for the Advancement of Science under a Creative Commons Attribution-NoDerivs 3.0 Germany License.

Zum 01.01.2015 ist eine Anpassung der Lizenzbedingungen (Entfall der Creative Commons Lizenzbedingung „Keine Bearbeitung") beabsichtigt, um eine Nachnutzung auch im Rahmen zukünftiger wissenschaftlicher Nutzungsformen zu ermöglichen.

On 01.01.2015 it is planned to change the License Conditions (the removal of the Creative Commons License condition "no derivative works"). This is to allow reuse in the area of future scientific usage.

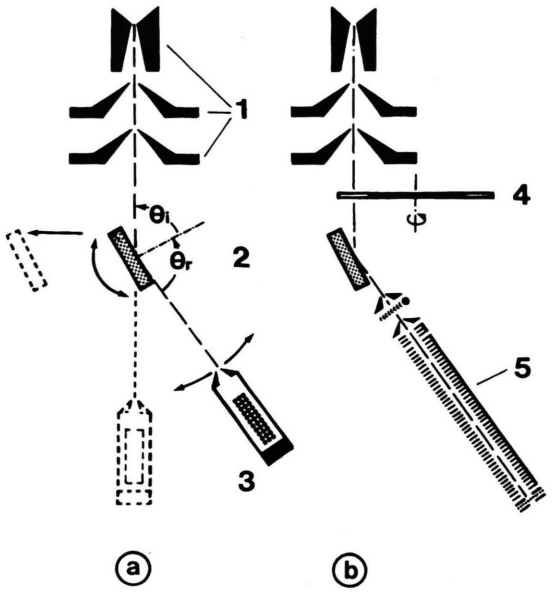

Fig. 1.1. Schematic view of the experimental setup (a) for measurements of the molecule flux and (b) for determinations of the velocity and the size of the clusters. The positions for incident beam measurements are represented in dashed lines. **1** beam generating system, **2** reflector (cp. Fig. 1.2), **3** ionization gauge tube, **4** chopper disk, **5** mass analyzer, θ_i angle of incidence, θ_r angle of reflection.

Table 1. Data of the nitrogen cluster beam in front of the reflector.

Flux density	$j_i = 6{,}9 \cdot 10^{19} \frac{N_2 - \text{molecules}}{cm^2\,s}$
Beam velocity	$v_i = 853 \frac{m}{s}$
Cluster size [13]	$\left(\frac{n}{z}\right)_i = 0{,}59 \cdot 10^6 \frac{N_2 - \text{molecules}}{\text{elementary charge}}$
Beam diameter d when using the	
optical reflector	3.1 mm
pressure-sensitive transistor	9.8 mm
gold-foil calorimeter	9.8 mm

rowest cross section, angle of aperture 10°, conus length 10 mm) and two pressure stages the beam gas expands from the inlet pressure $p_O = 8$ bar into the high vacuum (some 10^{-9} bar). The nozzle is in thermal contact with a cryostat filled with liquid nitrogen boiling at atmospheric pressure. Pulsed cluster beams of about 10 ms pulse-duration are generated by means of a fast-acting valve. The essential beam data are summarized in Table 1.

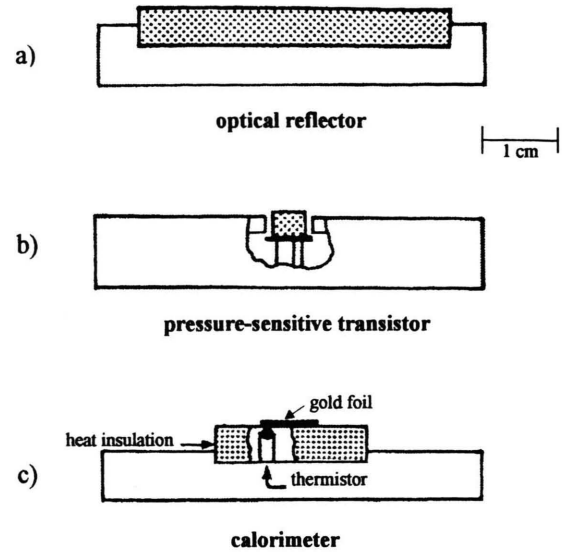

Fig. 1.2. Reflectors used (a) in the beam investigations, (b) in the momentum, and (c) in the energy transfer measurements.

The *flux density* is measured by a Pitot tube method. A modified ionization gauge tube (Leybold-Heraeus, Köln) is used [12]. The distance of its orifice from the point where the axis of the incident beam hits the reflector is 81 mm. By rotating the gauge tube around this point in the plane containing the axis of the incident beam and the normal of the reflector face (indicated by arrows in Fig. 1.1 a) the angular distribution of the reflected flux density in this plane is obtained. The angle of incidence θ_i can be varied by tilting the reflector. The position of the reflector and of the gauge tube for measurements performed on the incident beam without reflection is presented by dashed lines in Figure 1.1 a.

The *beam velocity* is determined by a time-of-flight measurement using the chopper disk. The *cluster size* is evaluated by an acceleration-field time-of-flight method [13]. The clusters are ionized by an electron beam normal to their path. By subsequent electrical acceleration of the clusters in the direction of their path a mass-dependent reduction in the time-of-flight is obtained. For reasons of apparatus design, the range of θ_i is limited to $45° \leqq \theta_i \leqq 90°$ in the time-of-flight measurements.

The various reflectors are shown in Figure 1.2. In the investigations performed on the reflected beam, the reflector is an optical stainless steel plate (*X5CrNi 18-9* "*Supra*", Zeiss, Oberkochen) with a polished area (40×16) mm^2 and a roughness depth of about 50 μm

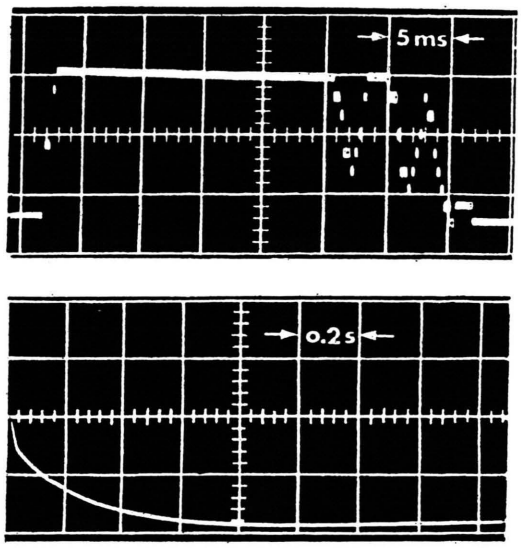

Fig. 2. (a) Output signal of the pressure sensitive transistor using a pulsed cluster beam of about 20 ms duration. The oscillations at the end of the pulse are caused by the closing of the valve (time base 5 ms).
(b) Output reading of the calorimeter using a miniature thermistor for the temperature measuring. The cluster beam gives rise to a cooling down of the reflector. Since the rise time of the calorimeter used exceeds the duration of the cluster beam (about 20 ms), the minimum of the temperature is reached after the cluster beam pulse is finished (time base 0.2 s).

(Figure 1.2. a). For $0° \leqq \theta_i \leqq 85°$ the cluster beam hits the reflector.

In the *momentum* transfer measurements carried out at the reflector, the stainless steel plate is replaced by the diaphragm of a pressure-sensitive transistor Stolab *Pitran PT-L2* (Figure 1.2b). The diaphragm consists of a Cu-Be-alloy, its surface being gold-plated. The diameter of the circular diaphragm is 4.75 mm. The transistor is sensitive in the direction normal to its surface. The pressure-sensitive transistor is used like a usual npn-transistor in common-emitter circuit with temperatur-stabilized operation point. A pressure difference between the upper and the bottom side of the diaphragm gives rise to a proportional output voltage. Due to the measuring of pressure *differences*, the influence of the absolute pressure in the high vacuum chamber is negligible. So, the pressure-sensitive transistor measures the momentum transfer normal to its surface during the cluster beam pulse. To eliminate the influence of a locally differing sensitivity, the active area of the transistor is completely covered by the cluster beam (Table 1). The reflector surface viewed by the beam and, hence,the impinging flux of molecules j are therefore proportional to the cosine of the angle of incidence θ_i:

$$j = j_O \cos \Theta_i \tag{1}$$

with j_O being the molecule flux at normal incidence ($\theta_i = 0°$).

The output voltage of the transistor is amplified (10...60 dB) and transmitted to the input of a digital averager (Data Lab. *DL 102 S*) with a capacity of 200 channels and a time resolution of 2 μs per channel. The averager is triggered by the valve of the cluster beam generating system. To compensate variations of the flux density, the averager produces a mean signal of eight cluster beam pulses. Figure 2a shows a typical output signal of the digital averager represented by an oscilloscope. For the evaluation, the height of the almost rectangular signal is taken from the oscillogram as a function of the angle of incidence. Therefore, the length of the cluster beam pulse is insignificant.

In the *heat transfer* measurements, a circular gold foil is used as reflector, having a thickness of 3 µm and a diameter of 7.21 mm (Figure 1.2c). It is mounted on a heat insulation and gives, together with a miniature thermistor (*K19,* Siemens), a sensitive calorimeter with a heat capacity of about 0.4 mJ/K. The heat insulation and the very thin wires of the thermistor with a diameter of 0.025 mm minimize heat leakages. The resistance of the thermistor is measured using a Wheatstone bridge, the output of which is almost proportional to the heat released from the calorimeter. Figure 2b shows the output signal of the Wheatstone bridge as a function of time. The minimum of the temperature of the calorimeter is reached after the cluster beam pulse is finished. This is caused by the time characteristics of the calorimeter, the rise time of which exceeds the length of the cluster beam pulse. Analogous to the pressure measurements, the output readings of the calorimeters are averaged using eight pulses, in each case. Thus, variations of the flux density of the incident beam are almost eliminated. In the heat transfer measurements the impinging flux is proportional to the cosine of the angle of incidence, as well (cf. (1)).

3. Results

3.1 Beam Measurements

3.1.1 Angular Distribution of the Flux Density

On a stepwise increase of the angle of incidence θ_i from 20° to 85°, the flux density shows a strong maxi-

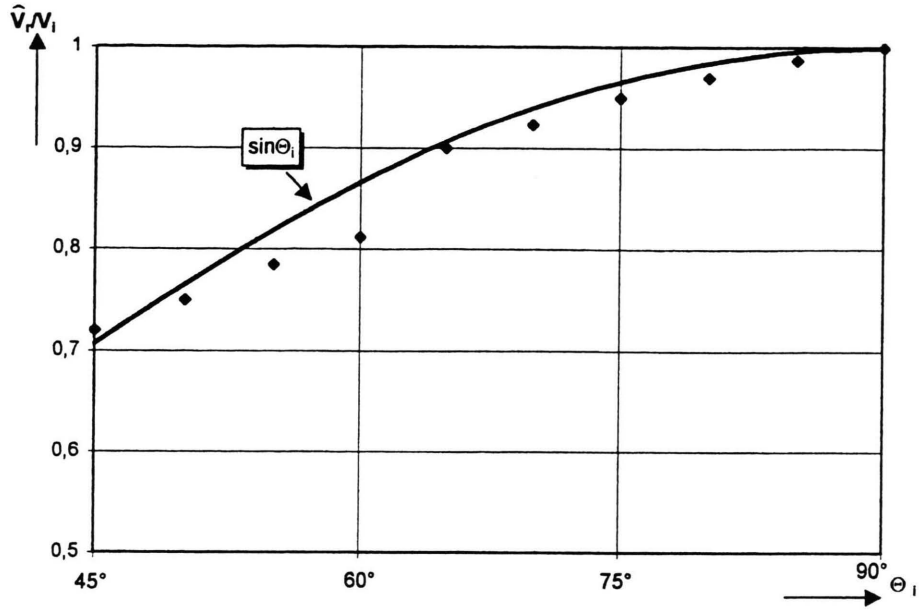

Fig. 3.1. Beam velocity $\hat{v}_r$ of the reflected beam in units of the velocity v_i of the incident beam as a function of the angle of incidence θ_i. The function $\sin\theta_i$ represents the normalized tangential component v_{it}/v_i of the velocity of the incident beam.

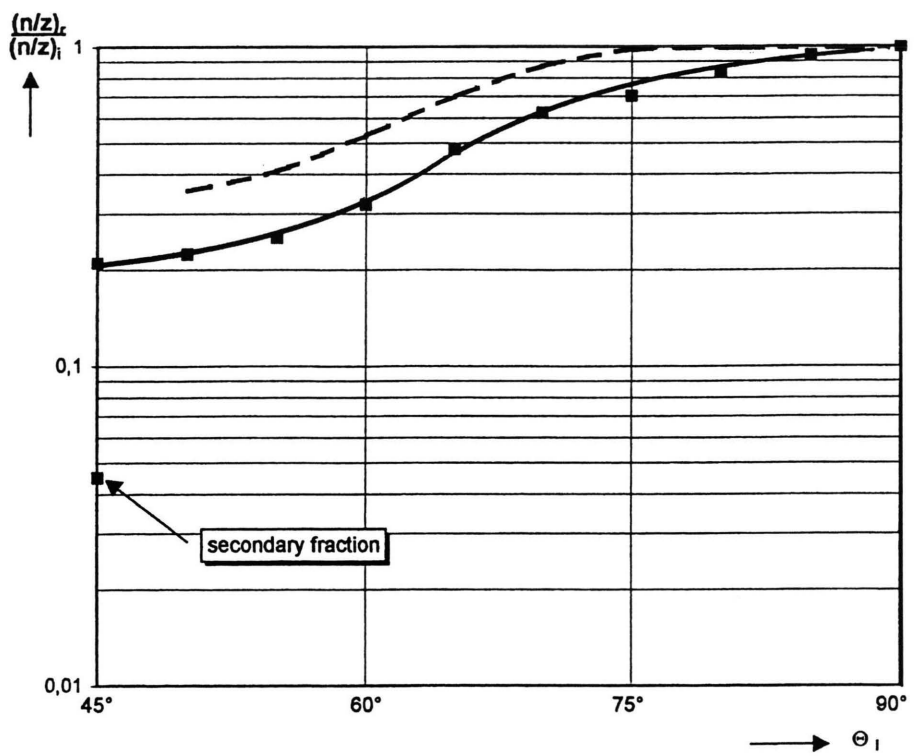

Fig. 3.2. Cluster size* $(n/z)_r$ of the reflected beam divided by the cluster size $(n/z)_i$ of the incident beam versus the angle of incidence θ_i. The dashed line represents the "reflection coefficient" (cf. **) taken from a previous paper. A secondary fraction is observed at an angle of incidence $\theta_i = 45°$.

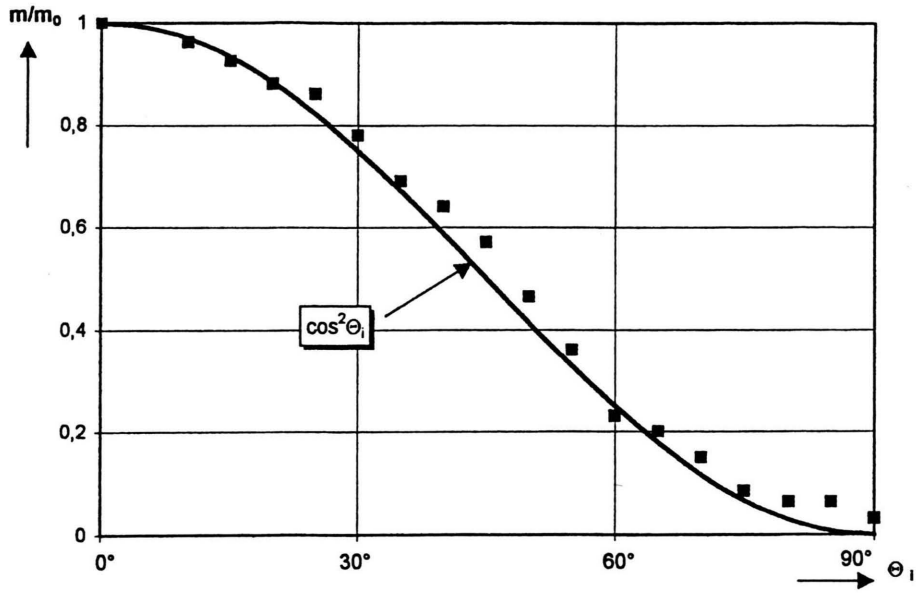

Fig. 4.1. Normal momentum flux m transferred to the reflector in units of the value m_O for normal incidence ($\theta_i = 0$) versus the angle of incidence θ_i. The flux of the impinging molecules is proportional to cos θ_i.

mum at a "most frequent" angle of reflection $\hat{\theta}_r \simeq 88°$. Thus, independent of the angle of incidence, the clusters leave the reflector almost tangentially. In other words, resolving the velocity v_r of the reflected beam into the components tangential and normal to he reflector surface v_{rt} and v_{rn}, respectively, this means that

$$v_{rt} \simeq v_r, \tag{2}$$

while the normal component nearly vanishes:

$$v_{rn} \simeq 0. \tag{3}$$

3.1.2 Beam Velocity Measurements

The beam velocity was always determined for the most frequent angle of incidence $\hat{\theta}_r \simeq 88°$ only. The time-of-flight is measured for the maximum of the time-of-flight distribution, and the corresponding "most frequent" beam velocity is determined. In Fig. 3.1 the most frequent velocity of the reflected beam $\hat{v}_r \simeq v_{rt}$, divided by that of the incident beam $v_i = 853$ ms^{-1}, is plotted versus the angle of incidence θ_i. The solid curve shows the function $\sin\theta_i$ representing the normalized tangential component of the velocity of the incident beam v_{it}/v_i. The approximate agreement of the measuring points with $\sin\theta_i$ proves that the tangential component is nearly maintained:

$$\hat{v}_{rt} \simeq v_{it}. \tag{4}$$

3.1.3 Cluster Size Measurements

The cluster size of the incident beam is determined by the acceleration-field time-of-flight method to be $(n/z)_i = 0.59 \times 10^6$ N_2-molecules/(elementary charge). Figure 3.2 shows in a logarithmic scale the cluster size of the reflected beam $(n/z)_r$ divided by $(n/z)_i$ as a function of the angle of incidence θ_i. While for great angles of incidence the cluster size of the reflected beam nearly agrees with that of the incident beam, a strong decrease is observed when the angle of incidence is reduced. Moreover, at $\theta_i = 45°$ a splitup of the reflected beam into two fractions is found, the flux density ratio of which is about 4:1. The velocity of the main fraction nearly agrees with the tangential velocity of the incident beam, while the velocity of the secondary fraction is by roughly 50% higher than that of the main fraction. The cluster size of the secondary fraction is about 20% of that of the main fraction. The dashed line in Fig. 3.2 represent the previously determined reflection coefficient**, which follows qualitatively the curve of the cluster size.

** "Reflection coefficient": If the flux density distributions are integrated over the solid range in which the readings of the Pitot tube are outside the limit of error and then divided by the incident flux, dimensionsless numbers are obtained, called reflection coefficient in [4].

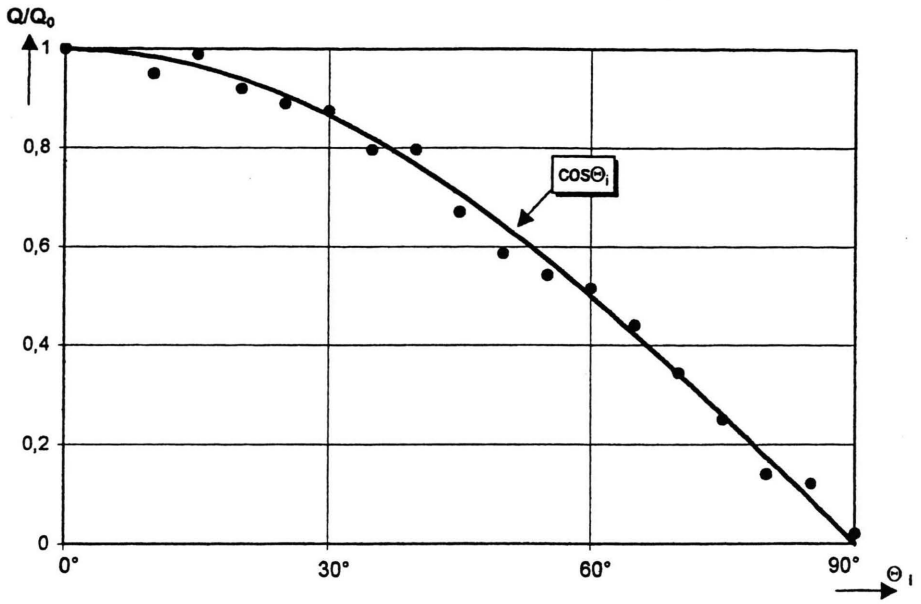

Fig. 4.2. Amount of heat Q released from the reflector in units of the value Q_O for normal incidence versus the angle of incidence θ_i. The flux of the impinging molecules is proportional to cos θ_i.

3.2 Reflector Measurements

3.2.1 Momentum Transfer

Figure 4.1 shows the readings of the pressure-sensitive transistor as a function of the angle of incidence θ_i. The fluxes m of the normal momentum are related to the flux m_O at normal incidence ($\theta_i = 0°$). The measuring points approximately agree with the function $\cos^2\theta_i$:

$$m/m_O \simeq \cos^2\theta_i. \tag{5}$$

Due to the coverage of the reflector, the impinging flux of molecules is proportional to $\cos\theta_i$ (cf. (1)). The momentum transferred to the reflector *per molecule* is, therefore, proportional to $\cos\theta_i$ and, hence, to the normal component of the velocity of the incident beam:

$$v_{in} = v_i \cos\theta_i. \tag{6}$$

3.2.2 Heat Transfer

Upon impingement of a cluster beam pulse, the gold foil reflector is remarkably cooled down. In Figure 4.2 the amount of heat Q released per beam pulse is plotted versus the angle of incidence θ_i. The curve of Q normalized to Q_O, the value for normal incidence ($\theta_i = 0°$), is well fitted by the function

$$Q/Q_O \simeq \cos\theta_i. \tag{7}$$

Since the reflector is completely covered by the cluster beam, the molecule flux to the reflector is proportional to $\cos\theta_i$. Therefore (7) indicates that the thermal energy q transferred *per molecule* is independent of the angle of incidence within the limit of error. For the gold foil reflector, the measured value q is about one third of the evaporation heat of macroscopical solid nitrogen per molecule.

4. Discussion

The determination of the angular distribution of the flux density and of the velocity of the reflected beam shows that during the reflection process nitrogen cluster beams largely lose the normal component of velocity, while the tangential component is almost preserved. This means that the clusters are reflected "inelastically". The tangential velocity of the clusters is insignificantly smaller than that of the incident beam, possibly be caused of friction processes.

The momentum transfer measurements reveal that the momentum flux normal to the reflector increases with

the cosine square of the incident angle; the momentum transferred per molecule, therefore, is proportional to the normal velocity of the incident beam. It can be seen from both the previously determined reflection coefficient and the mean cluster size measured here that with almost grazing incidence practically all the material hitting the reflector is found again in the reflected beam. Since the clusters leave the reflector almost tangentially, each molecule transfers only its *simple* normal momentum. So, the momentum fluxes measured here correspond to the inelastic component. For *small* angles of incidence with the clusters evaporating to a large extent, the measured values follow the *same* cosine square curve. That implies that even for the evaporated molecules being not detected in the reflected beam, the scattering process is inelastic in its character. This phenomenon could be explained by the assumption that during the reflection process the evaporated molecules form a gas layer between the base of the cluster and the reflector surface and effuse out of this gap, as out of a nozzle, mainly parallel to the reflector surface. According to this concept, the secondary fraction of small and fast agglomerates found at an incident angle of 45° could be formed by cluster fragments dragged by escaping molecules and accelerated in the direction of propagation.

Measurements of the cluster size show that the mean size of the agglomerates decreases monotonously with decreasing angle of incidence and, therefore, agrees qualitatively with the curve of the reflection coefficient. So, the reduction in the angle of incidence does not give rise to a more significant loss of whole clusters due to an increase in the visible extension of the mechanical defects of the reflector surface or a splitup of hitting clusters but rather causes a uniform diminution of *all* the clusters; however, the appearance of a secondary fraction at $\theta_i =$ 45° points out that cluster-splitup here takes place. The rough agreement of the molecule flux density ratio with the cluster size ratio indicates that the main fraction and the secondary fraction contains approximately the same number of agglomerates.

The fact that both the reflection coefficient and the cluster size decrease more than would have been expected from the mere conversion of kinetic energy of the clusters is explained by heat transfer from the reflector. The amount of heat released per molecule is independent of the incident angle within the limit of error, though it cannot be determined in the boundary case of grazing incidence because here the error limit approaches infinity.

The fact that the reflection coefficient exceeds the cluster size points out that in the evaluation of the reflected flux a portion of uncondensed molecules is measured, as well. This concept is supported by previous reflection measurements [4, 5] showing that the elevation of the background pressure in the high vacuum chamber causes a reduction of the reflection coefficient. In accordance with the momentum measurements, this implies that the evaporated molecules leave the reflector not isotropically but preferentially parallel to the reflector surface since, isotropic evaporation assumed, the molecules would not be detectable with the Pitot tube used. (For the broadening of the beam after its reflection in the direction normal to the plane of incidence and reflection cf. [4, 5]).

Acknowledgement

The author wishes to thank Professor E. W. Becker for his encouraging interest in this work.

The experiments were performed in 1971–1973 at the Institut für Kernverfahrenstechnik, Kernforschungszentrum Karlsruhe, Germany.

[1] E. W. Becker, K. Bier, and W. Henkes, Z. Phys. **146**, 333 (1959).
[2] E. W. Becker, R. Klingelhöfer, and P. Lohse, Z. Naturforsch. **17a**, 432 (1962).
[3] E. W. Becker, R. Klingelhöfer, and P. Lohse, Z. Naturforsch. **15a**, 644 (1960).
[4] E. W. Becker, R. Klingelhöfer, and H. Mayer, Z. Naturforsch. **23a**, 274 (1968).
[5] E. W. Becker, R. Klingelhöfer, and H. Mayer, represented at the 6th Intern. Symp. on Rarefied Gas Dynamics, Cambridge, Mass., USA 1969.
[6] E. W. Becker, J. Gspann, and G. Krieg, Entropie **30**, 59 (1969).
[7] J. Gspann and G. Krieg, represented at the 7th Intern. Symp. on Rarefied Gas Dynamics, Pisa 1970.
[8] G. Krieg, Thesis, Karlsruhe 1970.
[9] J. Gspann and G. Krieg, Verhandl. DPG (VI) **7**, 438 (1972).
[10] H. Mayer, Thesis, Karlsruhe 1972.
[11] H. Mayer, Z. Naturforsch. **28a**, 1733 (1973).
[12] R. Klingelhöfer and H. Röhl, Z. Naturforsch. **25a**, 402 (1970).
[13] J. Gspann and K. Körting, J. Chem. Phys. **59**, 4276 (1973).
[14] H. Falter, O. F. Hagena, W. Henkes, and H. v. Wedel, Int. J. Mass. Spectrum. Ion Phys. **4**, 145 (1970).